

Appendix C
By Isaac Storch
7/17/09

This document is a write-up of the data I took during the summer after my graduation, and is intended to be an appendix to my senior thesis, “Microwave Reset.” While there are still many problems left to solve, I hope these findings, along with my thesis, will provide a starting point for whoever continues work on the Microwave Reset.

The following data sets were taken on the same two well potential described in the body of the thesis. Based on the squid steps, a saddle point occurs at a 540 mV flux bias, and the two wells are symmetric at a 900 mV flux bias, so when I refer to the “operating bias” later, one has some idea of how deep the well is. Also, only three of the variables “start frequency”, “end frequency”, “duration”, and “rate” are independent, and when taking these data sets, “duration” was derived from the other three during the experiment. When most of the thesis data sets were taken, “rate” had been the derived variable.

We start by exploring the amplitude-rate phase locking phenomenon of Section 3.1 in more detail. Figure C.1 shows the phase locking threshold for three different operating biases on a log scale. Note that only a subset of the data follows the linear relationship predicted by autoresonance theory. The slopes average to 0.53 (including the fits on Fig. C.2). This number is closer to the predicted value of 0.75 than the thesis data, which gave 0.34. The slopes for different operating biases vary by about 8%, dramatically less than the simulated thresholds in Fig. 3.3. However, the linear regions on these plots correspond to chirp durations between 100 ns and 5 ns, while the thesis data sampled points with durations as long as 3000 ns. Also, the thesis data points were taken with even spacing in “duration” and not the log of “rate”, so the fitted theory curve had been weighted by the large number of points taken for low chirp rates. As we can see from Figs. C.1 and C.2, at low chirp rates the threshold no longer follows a linear curve. Thus a linear model was not a good representation of the thesis data (see Fig. 3.3).

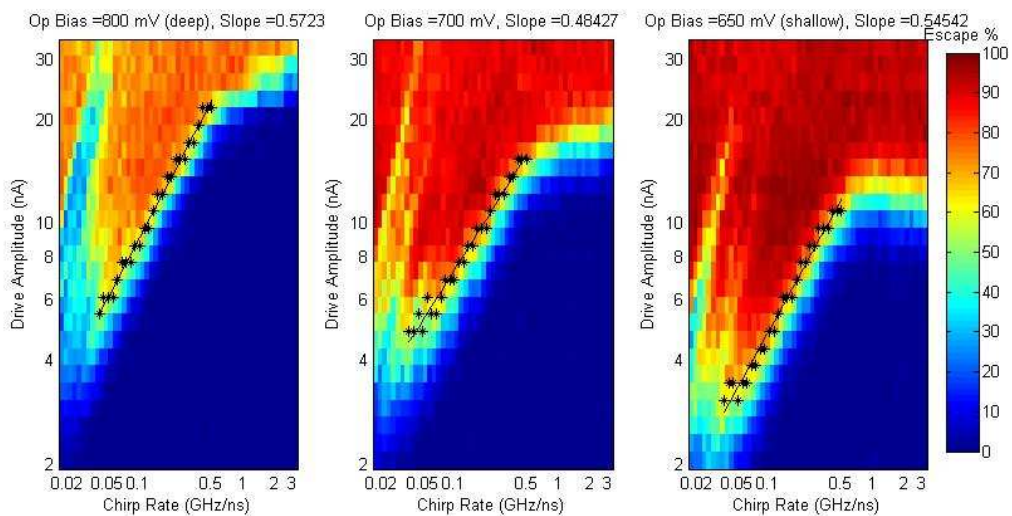


Figure C.1: Amplitude versus rate for various well depths (log scale). Start frequency = 7.315 GHz, end frequency = 3.91 GHz, and the resonant frequencies from left to right are 7.343 GHz, 6.672 GHz, 6.202 GHz. The y-intercepts from left to right are 3.5 nA, 3.1 nA, and 2.8 nA. The chirp durations that correspond to the limits on the chirp rate axis are calculated to be 201 ns and 1 ns. Note: some of the data taken at high chirp rates (the columns) is redundant because the DAC board can only create a chirp that is an integral number of nanoseconds in length, i.e. chirp rates that would give 0.8 and 1.2 ns chirps are experimentally the same as a 1 ns chirp.

In the thesis I suggested that the end frequency can always be eliminated as a variable by setting it as low as possible. However, this statement should be qualified. Figure C.3 shows end frequency versus start frequency plots for two different durations, the same kind of plot that provided the basis of my argument for keeping end frequency low (compare with Fig. 3.1). There are diagonal lines of lower escape probability that cut across these plots, which seems to imply that for this particular set of parameters, it is actually better to not set the end frequency to its lowest value. By observation, these lines correspond to specific chirp rates, which lie between 0.01 GHz/ns and 0.045 GHz/ns. One can see that these rates cover a region of low escape probability on the amplitude-rate plots in Fig. C.2 (the drive amplitude is 19.4 nA). However, note that from Fig. C.2 increasing the end frequency has little effect on the amplitude-rate behavior (lowering the start frequency does have an effect though). Thus, end frequency should be kept low for a given rate, not a given duration. If the reset is set up so that changing the end frequency also changes the rate, then the escape probability is harder to predict.

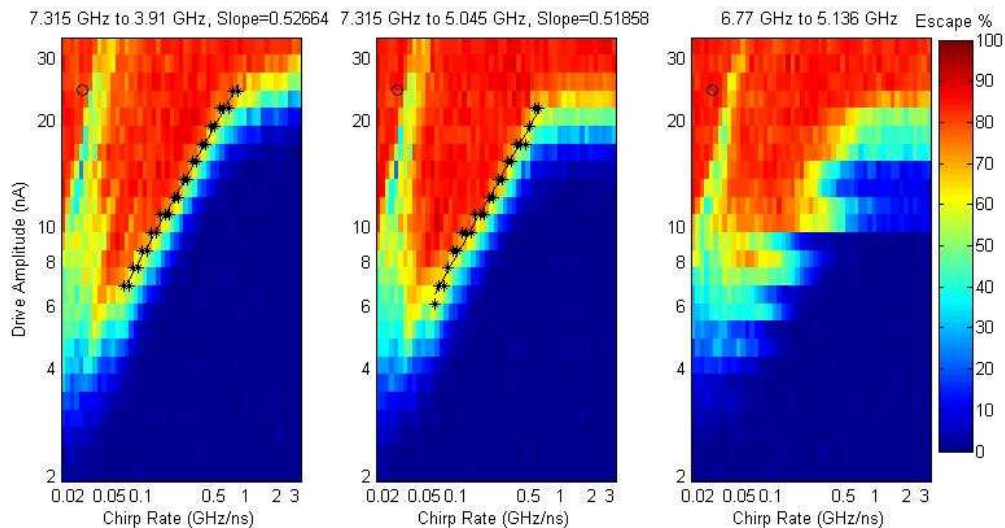


Figure C.2: Amplitude versus rate for various start and end frequencies (log-log scale). Operating bias = 750 mV, resonant frequency = 7.041 GHz. The start and end frequencies are given above each plot.

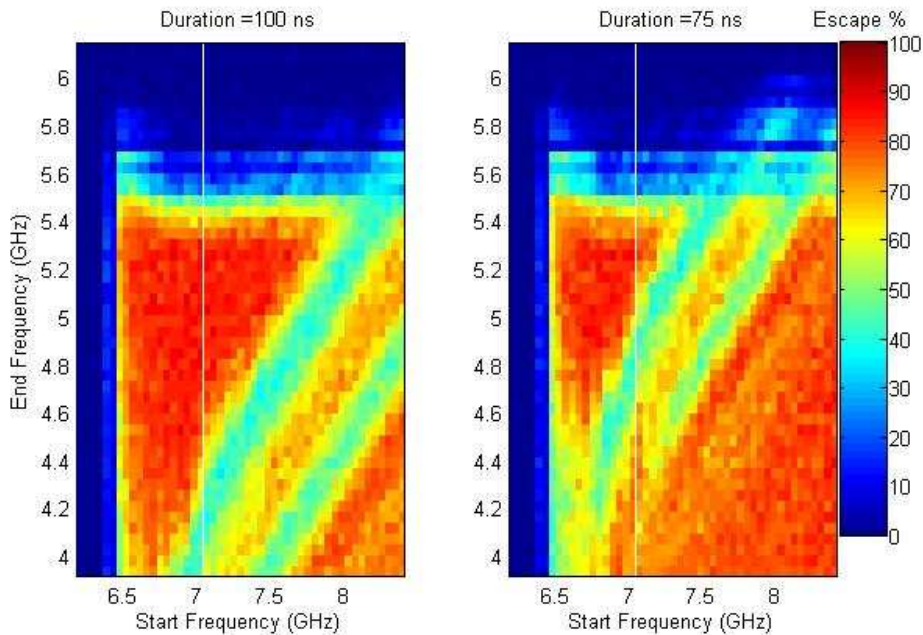


Figure C.3: End frequency versus start frequency for two different durations. The operating bias is 750 mV, and the attenuation is 10 dB (19.4 nA at the qubit).

In Section 3.2 I studied frequency selectivity by first making a 2D plot of start frequency versus attenuation, and then taking line cuts at various attenuations (Fig. 3.4). However, this process is overly complicated for determining frequency selectivity because a chirp with a given rate already has an attenuation that makes sense (one that puts it just above the phase locking threshold), so by sweeping attenuation we are looking at a lot of chirps that will not likely be used. For example, the start frequency versus attenuation plot shown in Fig. C.4 is like Fig. 3.4, except the rate is held constant instead of the duration. Looking up the rate on Fig. C.2 (0.0272 GHz/ns), one can choose an appropriate amplitude, which is marked by a small circle (24.4 nA or 8 dB attenuation). Considering again Fig. C.4, a line cut taken at 8 dB would look like a nice step function that demonstrates the frequency selectivity (difference in frequency between “not reset” and “reset”). Higher attenuations give lower escape probabilities, and at lower attenuations the frequency selectivity is negatively affected by small resonance peaks due to some unknown phenomenon. Thus, a simpler way to look at frequency selectivity is to choose both the amplitude and the rate based on plots like those in Fig. C.1, then make a 1D plot of escape probability versus start frequency.

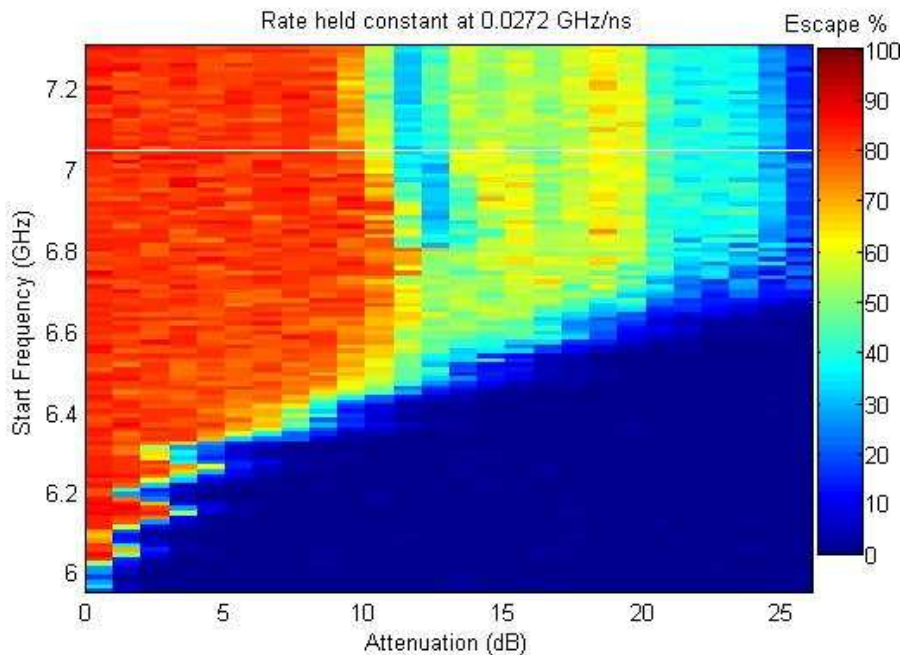


Figure C.4: Start frequency versus attenuation with the chirp rate fixed for all points. The operating bias is 750 mV (a line is drawn at the resonant frequency).

We will now use the aforementioned method for comparing the frequency selectivity of linear and quadratic chirps, and by “quadratic chirp” I mean a chirp with frequency $\omega(t) = \omega_0 - ct^2$. Figure C.5 shows the phase locking thresholds for linear and quadratic chirps at two different operating biases; the top two plots are quadratic chirps and the bottom two plots are linear chirps (note that the linear chirp plots are on a log scale). Three points were picked for frequency selectivity plots, which are shown in Fig. C.6. The blue, cyan, and green traces on Fig. C.6 correspond to the blue, cyan, and green circled points on Fig. C.5. Depending on what probabilities one chooses to define as “reset” and “not reset”, Fig. C.6 suggests there is little difference in frequency selectivity between using linear or quadratic chirps. However, what is interesting about the quadratic chirps is that the escape probability drops at high start frequencies. This makes sense because the quadratic chirp is a second order approximation to the ideal $\omega(t)$ shown in Fig. 1.7, and is thus more “fine tuned” to a particular start frequency. Hence, in a multiwell potential, a quadratic chirp would be useful for calibrating a separate chirp for each well, but a linear chirp would make more sense if one were going to design a single chirp for multiple wells.

It is also important to know if quadratic chirps are faster and/or require less power than linear chirps. Table C.1 shows the amplitude and duration for each of the circled chirps in Fig. C.5. One can see from this table that for the 750 mV operating bias, when quadratic and linear chirps have similar durations, the quadratic chirp has about a third less amplitude than the linear chirp, and when they have similar amplitudes, the quadratic chirp has about half the duration. However, for the 800 mV operating bias (a deeper well) the quadratic and linear chirps have about the same amplitude and duration.

Admittedly, this would be a better analysis if I had picked exactly the same amplitude or duration for all four of the blue/cyan/green points when I took the data. In any case, it might also be worthwhile to investigate other types of chirps, such as higher order polynomials or functions of time with non-integer powers.

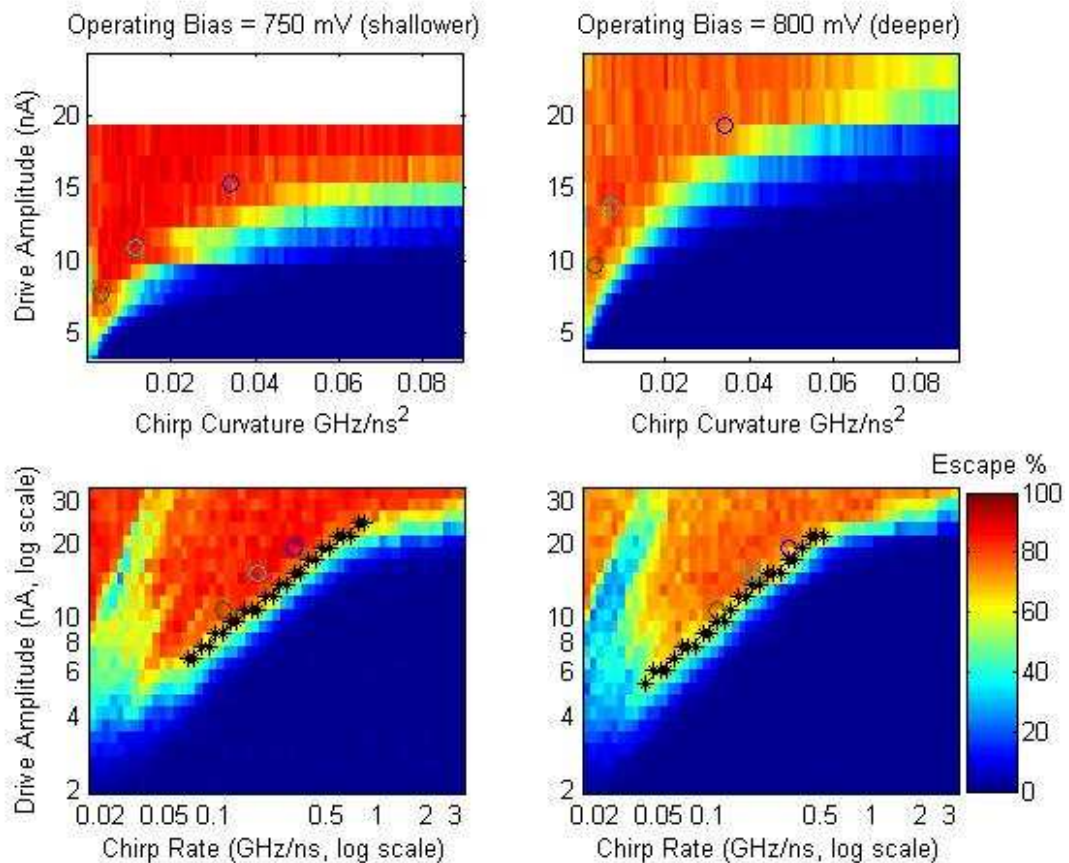


Figure C.5: Amplitude versus curvature and rate for two different operating biases. The top two plots are quadratic chirps and the bottom two plots are linear chirps. Top left: durations corresponding to limits of curvature axis = 114 ns to 6 ns; start frequency = 6.861 GHz. Top right: durations corresponding to limits of curvature axis = 122 ns to 6 ns; start frequency = 7.315 GHz. Bottom left: durations corresponding to limits of rate axis and limits of the linear region: 201 ns, 50 ns, 4 ns, 1 ns. For bottom right: 201 ns, 82 ns, 7 ns, 1 ns. Both bottom plots have start frequency = 7.315 GHz.

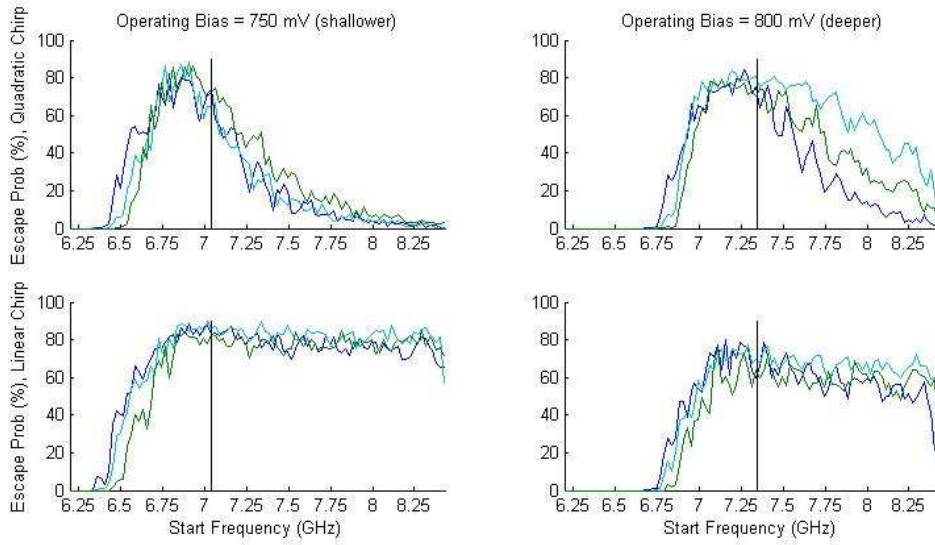


Figure C.6: These 1D sweeps correspond to the colored circles in Fig. C.5.

750 mV, quad, blue		750 mV, quad, cyan		750 mV, quad, green	
15.4 nA	9 ns	10.9 nA	16 ns	7.7 nA	29 ns
750, 800 mV, linear, blue		750, 800 mV, linear, cyan		750, 800 mV, linear, green	
19.4 nA	11 ns	15.4 nA	18 ns	10.9 nA	30 ns
800 mV, quad, blue		800 mV, quad, cyan		800 mV, quad, green	
19.4 nA	10 ns	13.7 nA	17 ns	9.7 nA	32 ns

Table C.1: Derived amplitudes and durations for the 12 selected chirps in Figs. C.5 and C.6.

We have deduced that quadratic chirps are more sensitive to the start frequency than linear chirps, but what about chirps that have both linear and quadratic components? (i.e. chirps of the form $\omega(t) = \omega_0 - c_1 t - c_2 t^2$) Figure C.7 shows color plots sweeping the linear and quadratic components with the attenuation, start and end frequencies fixed. The x-axis is purely linear chirps, while the y-axis is purely quadratic chirps. The right plot has a start frequency that is higher than would be ideal for a purely quadratic chirp. As we saw in Fig. C.6, the particle escapes for fewer quadratic chirps when the start frequency is increased, but the linear chirps continue to be able to make the particle escape. The transition between the plots in Fig. C.7 tells us that any positive quadratic component will make a linear chirp more sensitive to the start frequency.

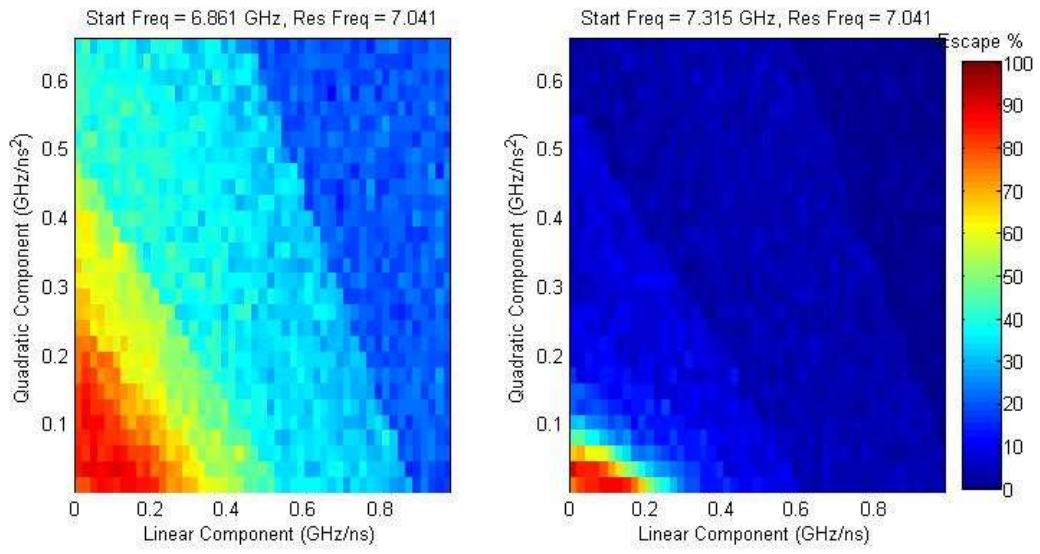


Figure C.7: Escape probability for combinations of quadratic and linear chirp components. Attenuation = 10 dB (19.4 nA), end frequency = 3.91 GHz, operating bias = 750 mV.